GVVPT2 Multireference Perturbation Theory Description of Diatomic Scandium, Chromium, and Manganese

ARTICLE *in* THE JOURNAL OF PHYSICAL CHEMISTRY A · APRIL 2012

Impact Factor: 2.69 · DOI: 10.1021/jp300401u · Source: PubMed

4 AUTHORS, INCLUDING:

Patrick K Tamukong
North Dakota State University
3 PUBLICATIONS **10** CITATIONS

THE JOURNAL OF PHYSICAL CHEMISTRY A

Article

pubs.acs.org/JPCA

GVVPT2 Multireference Perturbation Theory Description of Diatomic Scandium, Chromium, and Manganese

Patrick K. Tamukong, Daniel Theis, Yuriy G. Khait, and Mark R. Hoffmann*

Chemistry Department, University of North Dakota, Grand Forks, North Dakota 58202, United States

ABSTRACT: With relatively simple model spaces derived from valence bond models, a straightforward zero-order Hamiltonian, and the use of moderate-sized Dunning-type correlation consistent basis sets (cc-pVTZ, aug-cc-pVTZ, and cc-pVQZ), the second order generalized Van Vleck perturbation theory (GVVPT2) method is shown to produce potential energy curves (PECs) and spectroscopic constants close to experimental results for both ground and low-lying excited electronic states of Sc_2, Cr_2 and Mn_2. In spite of multiple quasidegeneracies (particularly for the cases of Sc_2 and Mn_2), the GVVPT2 PECs are smooth with no discontinuities. Since these molecules have been identified as ones that widely used perturbative methods are inadequate for describing well, due to intruder state problems, unless shift parameters are introduced that can obfuscate the physics, this study suggests that the conclusion about the inadequacy of multireference perturbation theory be re-evaluated. The ground state of Sc_2 is predicted to be $X^5\sum_u^-$, and its spectroscopic constants are close to the ones at the MRCISD level. Near equilibrium geometries, the $1^3\sum_u^-$ electronic state of Sc_2 is found to be less stable than the quintet ground state by 0.23 eV. The Cr_2 PEC has several features of the Rydberg−Klein−Rees (RKR) experimental curve (e.g., the pronounced shelf at elongated bond lengths), although the predicted bond length is slightly long (R_e = 1.80 Å with cc-pVQZ compared to the experimental value of 1.68 Å). The $X^1\sum_g^+$ ground state of Mn_2 is predicted to be a van der Waals molecule with a long bond length, R_e, of 3.83 Å using a cc-pVQZ basis set (experimental value = 3.40 Å) and a binding energy, D_e, of only 0.05 eV (experimental value = 0.1 eV). We obtained R_e = 3.40 Å and D_e = 0.09 eV at the complete basis set (CBS) limit for ground state Mn_2. Low lying excited state curves have also been characterized for all three cases (Cr_2, Mn_2, and Sc_2) and show similar mathematical robustness as the ground states. These results suggest that the GVVPT2 multireference perturbation theory method is more broadly applicable than previously documented.

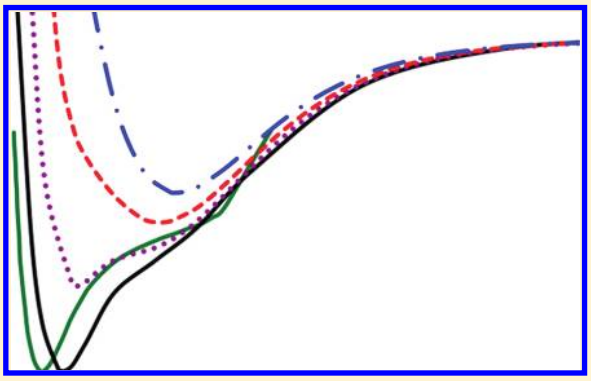

1. INTRODUCTION

Interest in transition metal (TM) chemistry has grown widely over the last few decades due in part to its applications in diverse areas such as catalysis, nanotechnology, and electronics.[1,2] In order to understand metals in large systems, it seems advantageous to thoroughly understand small clusters of a few atoms, beginning with dimers. Clearly, the properties of bulk materials cannot be predicted directly from those of the diatomic molecules or small clusters. The properties of bulk materials can, in general, be very different from those of their constituents. For example, the force constants of Sc_2, Cr_2, and Mn_2 are 0.76, 3.54, and 0.09 mdyn/Å, respectively. For the metal trimers, the values drop to 0.54 and 1.91 mdyn/Å for Sc_3 and Cr_3 respectively, but increases to 0.37 mdyn/Å for Mn_3.[3] Likewise, Mn_2 is generally accepted to be antiferromagnetic[4,5] (although recent ab initio calculations[6] with the self-consistent full-potential linearized augmented-plane-wave (FLAPW) method predicted Mn_2 to be ferromagnetically coupled with a local magnetic moment of 5 μ_B), whereas both Mn_4 and Mn_5 clusters are ferromagnetic.[7] The Mn_2 bond length has been determined experimentally to be 3.4 Å,[4] but in the bulk metal, the Mn−Mn distance is only 2.25−2.95 Å.[8]

Experimental studies on TMs are hampered by their very high melting and boiling points, leaving matrix isolation techniques as the best alternatives albeit with poor rotational spectra. Theoretical studies are complicated by the presence of many low-lying excited states.[9,10] The presence of partially filled d-subshells leads to several atomic terms and, consequently, several quasidegenerate molecular states. For example, the combination of ground state scandium (^2D_g; $4s^23d^1$) with either another ground state atom or one in one of the first three excited states (labeled as a^4F_g: $4s^13d^2$; a^2F_g: $4s^13d^2$; z^4F_u: $4s^14p^13d^1$) at only 1.427, 1.846, and 1.956 eV above the ground state already results in as many as 270 molecular states![11] The necessity to account for both static and dynamic electron correlation does not allow single-reference ab initio methods and density functional theory (DFT) to provide reliable descriptions of the bonding in TM diatomic molecules (see, for example, refs 12−15 and the references therein for an overview of DFT studies of Cr_2, Sc_2 and Mn_2, in which results

Received: January 12, 2012
Revised: April 7, 2012
Published: April 18, 2012

are dependent on the type of exchange-correlation functional used and some functionals predict species to be unbound).

Recent calculations by Camacho et al.[9] on the $X^1\sum_g^+$ ground state of Mn_2 at the MCQDPT (multiconfigurational quasidegenerate perturbation theory) and CASPT2 (complete active space second order perturbation theory) levels of theory revealed over 5000 intruder states, which did not allow for the construction of a smooth potential energy curve (PEC). Although the intruder state problem could be resolved by applying different level shift techniques, the spectroscopic constants obtained strongly depended on the type and size of the shift parameter. In the present paper, we investigate the applicability of the second-order generalized Van Vleck perturbation theory (GVVPT2),[16,17] which is not subject to problems from intruder states, is free of any parameters, and gives smooth continuous PECs for both ground and excited molecular electronic states, for Sc_2, Cr_2, and Mn_2.

The scandium dimer appears simple at first sight (i.e., only six valence electrons), but this observation is deceptive. Available experimental data for this molecule are quite fragmentary and disputable. By electron spin resonance (ESR) experiments, Knight et al.[18] established the ground state of Sc_2 as $X^5\sum_u^-$, which was later confirmed by Singer and Grinter[19] via magnetic measurements. From Raman vibrational spectroscopy, Moskovits et al.[20] determined the harmonic frequency and anharmonic constant of the ground state as ω_e = 238.9 cm^{-1} and $\omega_e x_e$ = 0.93 cm^{-1}. The equilibrium bond length in this state has not been measured but rather evaluated by Verhaegen et al.[21] as R_e = 2.70 Å (assuming that ω_e = 230 cm^{-1}). On the basis of mass spectrometric measurements, Verhaegen et al.[21] showed that the molecule is strongly bound and determined the binding energy of Sc_2 with respect to its ground state atoms (D_0^0) as 25.9 ± 5 kcal/mol (1.12 eV). Later, however, Verhaegen et al. revised this value as 38.0 ± 2.3 kcal/mol (1.65 eV) (see discussion in ref 11). Although the value of D_0^0 is still disputable,[11] the avoided crossing rule strictly ensures that the lowest $^5\sum_u^-$ state of Sc_2 correlates with the first excited asymptote $Sc(^2D_g)$ + $Sc(a^4F_g)$, and hence the dissociation energy (D_0) of ground state Sc_2 is equal to D_0^0 + 1.427 eV. Although many theoretical studies of Sc_2 have been performed and $1^5\sum_u^-$ is generally accepted as the ground state (see the review in ref 11), it has recently been disputed by Matxain et al.[22] Using the quantum diffusion Monte Carlo (DMC) method with Stuttgart relativistic pseudopotentials and basis sets (ECP10MDF), Matxain et al.[22] found the triplet state, $1^3\sum_u^-$, to lie 0.17 eV below the quintet $1^5\sum_u^-$ term. Although this ordering of states was corroborated by CASPT2 calculations (0.16 eV) performed by the same authors, they referred to these results as quite doubtful in their brief erratum.[23] More recent calculations of Sc_2, performed by Kalemos et al.[11] at the valence multireference internally contracted configuration interaction plus Davidson quadruple corrections (MRCI+Q) level with correlation consistent quadruple (cc-pVQZ) and quintuple zeta (cc-pV5Z) basis sets, agreed with the earlier result that $1^5\sum_u^-$ is the ground state and $1^3\sum_u^-$ is located (just 0.04 eV) above. The most recent calculations for ground state Sc_2 at the same level of theory, and using C_{2v} symmetry, but with extrapolation to the complete basis set (CBS) limit, have been performed by Kaplan and Miranda.[24]

The manganese dimer is also problematic for theorists. The ^6S ground state of the Mn atom ($3d^54s^2$) renders it quite stable with a high s−d excitation energy of 2.145 eV to the first ^6D excited state.[8,25] This is not surprising since electron promotion in this case occurs to one of the already occupied five d-orbitals, unlike the case of Sc ($3d^14s^2$) with a 5-fold degeneracy for the single electron in 3d (ignoring spin). The interaction of two ground state Mn atoms gives rise to 36 molecular states with multiplicities ranging from 1 to 11.[26] The ground state of the Mn_2 molecule has been found to be a van der Waals molecule with antiferromagnetically coupled 3d electrons.[4] From ESR measurements, Weltner et al.[4,7,27,28] reported the Mn_2 ground state as $X^1\sum_g^+$. A singlet ground state has been confirmed by resonance Raman spectra in rare gas matrices.[29] From Raman studies, Kirkwood et al.[25] reported an $X^1\sum_g^+$ ground state with constants ω_e = 68.1 cm^{-1} and $\omega_e x_e$ = 1.05 cm^{-1}. Various spectroscopic analyses gave dissociation energies in the range 0.02−0.15 eV,[30] and a bond length of 3.4 Å.[7]

Theoretical studies on electronic states of Mn_2, using MR perturbation methods, have encountered numerous problems varying from the discontinuity problem in constructing PECs[9,31,32] to poor convergence of perturbative expansions.[26] With the MCQDPT method, Camacho et al.[9] observed over 5000 intruders between 1.9 and 4.0 Å and a strong dependence of both the ground state PEC and spectroscopic constants on the shift parameters required to overcome the problem. This led to the authors questioning the adequacy of MRPT in tackling difficult systems such as the Mn_2 dimer.[9] At the MCQDPT2 level with the (18s15p8d4f2g)/[7s6p4d4f2g] basis set constructed from the (18s12p8d) set due to Koga et al.[33] augmented with the p-type primitives of Takewaki et al.[34] plus 4f2g polarization functions of Sekiya et al.,[35] Yamamoto and co-workers[32] obtained R_e = 3.29 Å, D_e = 0.14 eV, and ω_e = 53.46 cm^{-1} for the $X^1\sum_g^+$ ground state of Mn_2. Using second- and third-order *n*-electron valence state perturbation theory (NEVPT2 and NEVPT3) and the atomic natural orbitals (ANO) relativistic correlation consistent basis set developed by Roos et al.[36] and with the inclusion of scalar relativistic corrections through the Douglas−Kroll−Hess (DKH) Hamiltonian, Angeli and co-workers[37] obtained R_e = 3.71 Å, D_e = 0.08 eV, and ω_e = 41.0 cm^{-1} in the case of NEVPT2, and R_e = 3.82 Å, D_e = 0.07 eV, and ω_e = 43.0 cm^{-1} with NEVPT3. At the MRCI level with the use of the aug-cc-pVQZ basis set, Buchachenko et al.[26] obtained R_e = 3.82 Å, D_e = 0.05 eV, and ω_e = 33.7 cm^{-1}, while Tzeli et al.[8] obtained R_e = 3.80 Å, D_e = 0.05 eV, ω_e = 36 cm^{-1}, and R_e = 3.64 Å, D_e = 0.06 eV, ω_e = 42 cm^{-1} at the MRCI+Q and average coupled pair functional (ACPF) levels with the same basis, respectively. DFT studies on Mn_2 gave contradictory results,[38−43] most of which favor, in contrast to ab initio wave function methods, a high spin (S = 5) ground state.

Although diatomic chromium was first identified over four decades ago,[44,45] the bonding in this molecule remains a formidable challenge to theoretical chemists. Over 40 different computational treatments have been made on Cr_2 in an effort to elucidate its bonding. Early attempts did not lead to useful characterizations and resulted in published statements such as that by Salahub in 1987 that labeled Cr_2 as "a bête noire".[46] Bauschlicher and Partridge in 1994 declared that "obtaining a quantitative description of Cr_2 has so far proven to be impossible",[47] while in as late as 1999 Thomas et al.[14] stated that "it has been found repeatedly that improving the computational level did not necessarily improve the results".

By resonant two-photon ionization (R2PI) spectroscopy, Michalopoulos et al.[48] determined the bond length of Cr_2 to be R_e = 1.68 ± 0.01 Å and its ground state as $X^1\sum_g^+$. By laser-

dx.doi.org/10.1021/jp300401u | J. Phys. Chem. A 2012, 116, 4590−4601

induced fluorescence spectroscopy, Bondybey et al.[49] determined the equilibrium bond length to be R_e = 1.679 Å with a harmonic frequency of ω_e = 470 cm^{-1}. From photoionization spectroscopy, Simard et al.[50] obtained a dissociation energy D_e of 1.56 ± 0.06 eV, while the mass spectrometric experiment by Hilpert and Ruthardt[51] led to D_e = 1.473 ± 0.056 eV, and Su et al.[52] reported D_e = 1.45 ± 0.10 eV. By negative ion photoelectron spectroscopy, Casey and Leopold[53] determined the ground state harmonic frequency of Cr_2 to be approximately ω_e = 481 cm^{-1}. In this experiment, they obtained transition energies from 29 vibrational levels and, using the Rydberg−Klein−Rees (RKR) method,[54−56] obtained a PEC for the ground state of Cr_2 that clearly showed a shelf region from around 2.5 Å to 3.0 Å. Theoretical efforts on ground state Cr_2 are assessed relative to this RKR PEC. Early attempts gave disappointing results. Coupled cluster with single and double excitation (CCSD) calculations[57] with the (14s11p6d2f1g)/[10s8p3d2f1g] basis set gave a too short bond length (R_e = 1.46 Å) and a too large harmonic frequency (ω_e = 1161 cm^{-1}). At the unrestricted CCSD level with perturbative inclusion of triples [UCCSD(T)], Bauschlicher and Partridge,[47] using the (20s15p10d6f4g)/[9s8p7d5f2g] basis set, obtained R_e = 2.54 Å and D_e = 0.89 eV. With a CASSCF reference function and then an Epstein-Nesbet second-order perturbation correction using the [10s8p3d2f] basis set, a reasonably good (R_e = 1.6258 Å) bond length was obtained, but the potential function could not dissociate properly (D_e = 2.786 eV).[58] With the multireference ACPF (MRACPF) formalism using the (20s15p10d6f)/[9s8p7d5f] basis set,[47] Dachsel et al.[59] obtained R_e = 1.72 Å, D_e = 1.09 eV, and ω_e = 338.7 cm^{-1}. In contrast to earlier disappointing CASPT2 studies,[60,61] Roos[62] performed very large CASPT2 calculations that considered an expanded active space of 12 electrons and 16 molecular orbitals (MOs; derived from the 3d and 4s subshells plus all bonding MOs from 4p and the corresponding antibonding sigma type), used the modified (g1) zero-order Hamiltonian of Andersson,[63] a large ANO basis set, relativistic corrections, and level shifts, and obtained good values for the bond length, R_e = 1.66 Å, and harmonic frequency, ω_e = 450 cm^{-1}, but somewhat overestimated the dissociation energy, D_e = 1.68 eV. Calculations done later at the CIPT2[64] level (N.B. a hybrid of multireference configuration interaction and second order multireference perturbation theory), using the [9s8p7d7f5g3h] basis set, gave values of R_e = 1.756 Å, D_e = 1.18 eV, and ω_e = 322 cm^{-1}. The same authors performed calculations at the CASPT2 and MRCI+Q levels with the same basis set and reported R_e = 1.678 Å, D_e = 1.84 eV, and ω_e = 565 cm^{-1} for CASPT2 and R_e = 1.664 Å, D_e = 1.01 eV, and ω_e = 511 cm^{-1} for MRCI+Q. Notably, none of these three studies gave the correct dissociation energy. Essentially more accurate (though very costly) results were obtained by Müller[65] at the fully uncontracted multireference averaged quadratic coupled cluster (MR-AQCC) level. With the use of a large flexible basis set (including h and i functions), with 28 correlated electrons (3s, 3p, 3d, and 4s electrons) generating up to 2.8 billion configuration state functions (CSFs) and by accounting for scalar relativistic effects through the use of the DKH Hamiltonian,[66,67] he obtained R_e = 1.685 Å, D_e = 1.48 eV, and ω_e = 459 cm^{-1} after extrapolation to the CBS limit. Surprisingly, his results are poor with the use of a triple-ζ basis set (TZP), giving two shallow minima at 1.758 Å and 2.5 Å with almost the same energy (−0.078 eV).

The most recent calculations on Cr_2 were performed by Hongo and Maezono,[68] Ruipérez et al.,[69] and Kurashige and Yanai.[70] Calculations at the variational Monte Carlo (VMC) and DMC levels overestimated R_e by over 25% and underestimated D_e by some 40%.[68] Ruipérez et al.[69] performed calculations at the restricted active space second order perturbation theory (RASPT2) and CASPT2 levels using the (21s15p10d6f4g)/[10s10p8d6f4g] basis set of Roos[62] and exploiting two different zero-order Hamiltonians. The RASPT2 PEC proved to be seriously deficient at long distances, and the CASPT2 calculations with the g1 zero-order Hamiltonian overestimated D_e by 0.6 eV. In the case of using a zero-order Hamiltonian with the ionization potential-electron affinity (IPEA) shift, these authors observed a strong dependence of the CASPT2 PEC on the IPEA shift parameter, and no value was found that consistently gave the best results in terms of shape of the PEC and spectroscopic constants. Whereas the best estimate for IPEA giving a PEC with a shape that agreed well with experiment was 0.45, the best IPEA value for predicting the right R_e was 0.50; for D_e, it was 0.45, and for $\Delta G_{1/2}$, it was 0.40. Kurashige and Yanai[70] performed analogous CASPT2 calculations but with a density matrix renormalization group SCF (DMRG-SCF) reference function, constructed within the active space (12e, 28o) derived from the 3d, 4s, 4p, and 4d subshells, and using the cc-pwCV5Z basis set. After a linear extrapolation to infinite size of the renormalized basis sets, Kurashige and Yanai,[70] using a zero-order Hamiltonian with an IPEA shift of 0.25 au, obtained the following very good results: R_e = 1.682 Å, D_e = 1.551 eV, and ω_e = 471 cm^{-1}. However, the same calculations without any shift led to less satisfactory results: R_e = 1.719 Å, D_e = 1.337 eV, and ω_e = 361 cm^{-1}, which corroborates the previously noted sensitivity to shift parameters.

The main goal of the present work is to investigate the characteristics and especially the accuracy of the GVVPT2 method, which is free of any parameters, for describing complicated TM systems, using relatively small active spaces based on conventional chemical notions of valence orbitals. While GVVPT2 PECs must be smooth and continuous, based on formal arguments, a key point of assessment will be whether the PECs of both ground and excited states are free from artificial inflection points, i.e., "wiggles". The rest of the paper is organized as follows: Section 2 briefly reviews the salient features of GVVPT2 and describes details as to how the calculations were done, the results are presented and discussed in Section 3, and a final section concludes the paper.

2. METHODOLOGY

2.1. GVVPT2 Method. Here, we briefly describe important features of GVVPT2 relevant to the present study (for details on the formulation and high-performance implementation of GVVPT2, see refs 16, 17, and 71−75 and the references therein). In GVVPT2, the total Hilbert space is partitioned into a model space, L_M (generally of an MCSCF type), and an external space (L_Q) whose configurations are related to the model space CSFs by single and double electron excitations. The model space is further partitioned into a primary space (L_P), spanned by a set of reference functions (typically the lowest MCSCF states), and its orthogonal complement, called the secondary space (L_S), which constitutes a "buffer zone" between the primary and external spaces. Only states in the primary subspace are perturbatively corrected, but states in both the primary and secondary subspaces are considered in the

dx.doi.org/10.1021/jp300401u | J. Phys. Chem. A 2012, 116, 4590−4601

final diagonalization of the effective Hamiltonian in the total model space. The buffer zone energetically separates the primary and external spaces sufficiently for primary−external (P−Q) interactions to be described perturbatively, while circumventing most intruder state problems. The intruder state problem is an "Achilles's heel" for multireference perturbation theory methods and has generated different attempts to resolve the problem, such as the use of shift techniques or elimination of offending states. Moreover, attempts to circumvent the problem by changes in active spaces are commonly used. Unfortunately, these approaches do not work well in all situations, as demonstrated recently by Camacho et al.[9] for the case of Mn_2 and Ruipérez et al.[69] for the case of Cr_2. The use of a Dyall bielectronic zero-order Hamiltonian, as in NEVPT2,[76,77] seems to deal well with intruder states, albeit with a significant increase in complexity relative to one-electron Hamiltonians. By using nonlinear denominator shifts that vary continuously, the GVVPT2 method avoids the intruder state problem completely and guarantees smooth continuous PECs for both ground and excited electronic states, even for cases with several quasidegeneracies, as typical of TM systems. Moreover, the nonlinear denominator shifts allow the use of smaller, in some cases significantly so, model spaces, since the requirement for fairly large separation of model and external spaces required for linear-resolvent-based multireference perturbation theories is mitigated. The nonlinear denominator shifts in GVVPT2 are realized by the use of a resolvent that is both degeneracy-corrected and contains a hyperbolic tangent function as a switching function from nondegenerate to degenerate regimes.[16] The choice of $\tanh(x)$ as a switching function was not happenstance but dictated by four strict mathematical conditions to be satisfied.[16] Moreover, although one formally could use $\tanh(\lambda x)$ with parameter $\lambda > 0$, test calculations showed that results were only weakly sensitive to a choice of this parameter,[16] and GVVPT2 was defined with $\lambda = 1$. Note also that the GVVPT2 method supports both complete and incomplete model spaces, is subspace-specific, and is inherently spin-adapted. Thus, it is capable of treating electronic states while maintaining a pure total spin quantum number, avoiding the nuisance of spin contamination.

2.2. Computational Details. The macroconfiguration approach[78] was used within the GVVPT2 method in all calculations. In the macroconfiguration formalism, the active space is partitioned into orbital groups following physical intuition, and restrictions are imposed on group occupancies. Each unique assignment of electrons to active orbital groups constitutes one macroconfiguration (MCRM). This is to be distinguished from a normal electron configuration that specifies the electronic occupation numbers of individual orbitals. Furthermore, the macroconfiguration approach permits a huge number of noninteracting electronic configuration pairs to be screened and, moreover, provides an efficient way of regenerating excited configurations. Each MCRM generates a unique set of configurations that are orthogonal to configurations of other MCRMs.

Because the macroconfiguration approach entails essentially unlimited flexibility, subject to computational resource constraints, constructing the appropriate model space often requires some experimentation. However, there are design principles and diagnostics that facilitate construction. In general, a principal desideratum is that the accuracy of the calculation is constant across the range of the potential energy surface (or curve, for a diatomic molecule) of interest. For the present study, this requires the ability to dissociate correctly for each curve of interest, which suggests that construction begins from a valence bond description. Symmetry constraints are powerful criteria on which to assess adequacy, irrespective of specific numerical results, and were actively used in the present study. Lastly, because GVVPT2 is mathematically and computationally robust (i.e., there will always be a solution to the equations, even when the accuracy is diminished), wave function amplitudes can be analyzed for the presence of large individual contributions from the external space, which signal the need to include additional macroconfigurations and/or orbitals in the model space. Obviously, obtaining such a result after a significant portion of the potential energy surface has been studied is disappointing and a waste of computational resources; consequently, assessments of model space adequacy are optimally made for a few selected points across the potential energy surface of interest prior to extensive calculations. However, in the situation that convergence of the underlying MCSCF calculations is nontrivial, and use is made of the availability of orbitals from adjacent geometries, one can encounter problems with the model space only after a significant number of calculations with an inadequate model space have been made. In this paper, taking into account the difficulties of prior studies of the subject molecules that included struggles to find adequate model spaces (even when using CASSCF), we describe the results from a select subset of the model spaces that were used and not just those from the eventually best ones.

For all three cases (Sc_2, Cr_2, and Mn_2), the active space consisted of valence orbitals derived from atomic 3d and 4s subshells in the cases of Sc_2 and Cr_2 and some of the studies of Mn_2; for other studies of Mn_2, the 4s-derived MOs were put into the active core. With these active orbitals, MCRMs were constructed as follows.

For Cr_2, a single-reference MCRM was defined by distributing 12 active electrons among six active orbital groups, with each group consisting of a bonding MO and its corresponding antibonding counterpart as follows:

$$(3d_{xz}\pi_u 3d_{xz}\pi_g^*)^2(3d_{yz}\pi_u 3d_{yz}\pi_g^*)^2(3d_{z^2}\sigma_g 3d_{z^2}\sigma_u^*)^2$$
$$(3d_{x^2-y^2}\delta_g 3d_{x^2-y^2}\delta_u^*)^2(4s\sigma_g 4s\sigma_u^*)^2(3d_{xy}\delta_g 3d_{xy}\delta_u^*)^2$$

This reference MCRM was used to investigate the PECs of the $X^1\sum_g^+$, $1^3\sum_u^+$, $1^5\sum_g^+$, and $1^7\sum_u^+$ electronic states of Cr_2.

For Sc_2, two sets of reference MCRMs were used in separate calculations. In the first set, each active MO and its corresponding antibonding counterpart constituted a group, except that the four σ MOs dominated by $3d_z^2$ and 4s were placed in one subspace. Two reference MCRMs (labeled Case 1 in Figure 1 and Table 1 in the Results and Discussion section) were defined from this grouping (and used to compute the $X^5\sum_u^-$state), viz.,

$$(3d_{xz}\pi_u 3d_{xz}\pi_g^*)^1(3d_{yz}\pi_u 3d_{yz}\pi_g^*)^1$$
$$(3d_{z^2}\sigma_g 3d_{z^2}\sigma_u^* 4s\sigma_g 4s\sigma_u^*)^4(3d_{x^2-y^2}\delta_g 3d_{x^2-y^2}\delta_u^*)^0$$
$$(3d_{xy}\delta_g 3d_{xy}\delta_u^*)^0$$

dx.doi.org/10.1021/jp300401u | J. Phys. Chem. A 2012, 116, 4590−4601

$$(3d_{xz}\pi_u 3d_{xz}\pi_g^*)^1(3d_{yz}\pi_u 3d_{yz}\pi_g^*)^1$$
$$(3d_{z^2}\sigma_g 3d_{z^2}\sigma_u^* 4s\sigma_g 4s\sigma_u^*)^2(3d_{x^2-y^2}\delta_g 3d_{x^2-y^2}\delta_u^*)^1$$
$$(3d_{xy}\delta_g 3d_{xy}\delta_u^*)^1$$

The superscripts denote the number of electrons assigned to each group of MOs. For the second set of reference MCRMs (labeled Case 2 in Figure 1 and Table 1 in the Results and Discussion section), the MOs were grouped according to orbital type (π, σ, and δ), and six active electrons were distributed among the three orbital groups resulting in five reference MCRMs, viz.,

$$(3d_{xz}\pi_u 3d_{xz}\pi_g^* 3d_{yz}\pi_u 3d_{yz}\pi_g^*)^2(3d_{z^2}\sigma_g 3d_{z^2}\sigma_u^* 4s\sigma_g 4s\sigma_u^*)^4$$
$$(3d_{x^2-y^2}\delta_g 3d_{x^2-y^2}\delta_u^* 3d_{xy}\delta_g 3d_{xy}\delta_u^*)^0$$

$$(3d_{xz}\pi_u 3d_{xz}\pi_g^* 3d_{yz}\pi_u 3d_{yz}\pi_g^*)^1(3d_{z^2}\sigma_g 3d_{z^2}\sigma_u^* 4s\sigma_g 4s\sigma_u^*)^4$$
$$(3d_{x^2-y^2}\delta_g 3d_{x^2-y^2}\delta_u^* 3d_{xy}\delta_g 3d_{xy}\delta_u^*)^1$$

$$(3d_{xz}\pi_u 3d_{xz}\pi_g^* 3d_{yz}\pi_u 3d_{yz}\pi_g^*)^2(3d_{z^2}\sigma_g 3d_{z^2}\sigma_u^* 4s\sigma_g 4s\sigma_u^*)^3$$
$$(3d_{x^2-y^2}\delta_g 3d_{x^2-y^2}\delta_u^* 3d_{xy}\delta_g 3d_{xy}\delta_u^*)^1$$

$$(3d_{xz}\pi_u 3d_{xz}\pi_g^* 3d_{yz}\pi_u 3d_{yz}\pi_g^*)^1(3d_{z^2}\sigma_g 3d_{z^2}\sigma_u^* 4s\sigma_g 4s\sigma_u^*)^3$$
$$(3d_{x^2-y^2}\delta_g 3d_{x^2-y^2}\delta_u^* 3d_{xy}\delta_g 3d_{xy}\delta_u^*)^2$$

$$(3d_{xz}\pi_u 3d_{xz}\pi_g^* 3d_{yz}\pi_u 3d_{yz}\pi_g^*)^2(3d_{z^2}\sigma_g 3d_{z^2}\sigma_u^* 4s\sigma_g 4s\sigma_u^*)^2$$
$$(3d_{x^2-y^2}\delta_g 3d_{x^2-y^2}\delta_u^* 3d_{xy}\delta_g 3d_{xy}\delta_u^*)^2$$

This set of five reference macroconfigurations was used to construct the PECs for the $X^5\sum_u^-$, $1^3\sum_u^-$, and $1^3\sum_g^-$ electronic states of Sc_2.

For Mn_2, four reference model spaces consisting of single MCRMs were used in separate calculations (labeled Cases A–D in Table 4 and Figures 6–8 in the Results and Discussion section). The first reference model space (Case A), used to investigate the $X^1\sum_g^+$ state of Mn_2, consisted of a MCRM similar to that for Cr_2, except that all σ MOs were grouped together, and six active electrons were assigned to the σ subspace. The second reference model space (Case B) consisted of a MCRM obtained by further increasing the model space within the 3d/4s manifold by grouping all π MOs in one subspace. In the next set of calculations, $3p_z$-derived σ MOs were included into the sigma subspace of the second reference model space to give the following MCRM (Case C):

$$(3d_{xz}\pi_u 3d_{xz}\pi_g^* 3d_{yz}\pi_u 3d_{yz}\pi_g^*)^4(3p_z\sigma_g 3p_z\sigma_u^* 3d_{z^2}\sigma_g 3d_{z^2}\sigma_u^* 4s\sigma_g 4s\sigma_u^*)^{10}$$
$$(3d_{x^2-y^2}\delta_g 3d_{x^2-y^2}\delta_u^*)^2(3d_{xy}\delta_g 3d_{xy}\delta_u^*)^2$$

Lastly, a reference model space obtained from an MCRM similar to that for Cr_2 in which the 4s- derived MOs were removed from the active space and included with 3s and 3p-dominated MOs in the active core was used (Case D).

With the reference MCRMs described above, multiconfigurational self-consistent field (MCSCF) calculations were performed to account for static electron correlation. The initial MO guesses for one geometry were obtained from approximate natural orbitals of second-order restricted Møller–Plesset perturbation (RMP2) calculations from a closed-shell Hartree–Fock (HF) reference; subsequent MCSCF calculations used orbitals from adjacent geometries. Dynamic electron correlation energy was accounted for through GVVPT2 calculations. In addition to all active space electrons, high-lying core orbitals (i.e., 3s and 3p electrons plus the four 4s electrons of Mn for Case D) were all correlated at the GVVPT2 level of theory. All calculations were done using the D_{2h} point group (i.e., the largest point group available in the UNDMOL 1.1 suite of programs: an electronic structure software suite developed and maintained at the University of North Dakota).

For all calculated states of Sc_2, the correlation consistent triple-ζ (cc-pVTZ) basis set,[79] consisting of 151 Gaussian primitives contracted to [7s6p4d2f1g], was employed. Calculations on all states of Cr_2 were done with the cc-pVTZ basis set, but a number of other basis sets were explored in calculations on the Cr_2 ground state PEC. These included the correlation consistent quadruple-ζ (cc-pVQZ) basis[79] built from 202 primitive Gaussians and contracted to [8s7p5d3f2g] (N.B. the h-functions were neglected in all calculations employing this basis set), the aug-cc-pVTZ basis[79] consisting of 186 primitive Gaussians contracted to [8s7p5d3f2g], and several effective core potential (ECP) basis sets: Stuttgart Relativistic Small Core (RSC) 1997 ECP,[80−82] Los Alamos National Laboratory double and triple-ζ ECPs, that is, LANL2DZ[83] and LANL08.[84,85] The performance of these basis sets on the Cr_2 ground state PEC is shown in Figures 2 and 3 in the Results and Discussion section. Calculations on all electronic states of Mn_2 were done with the cc-pVTZ basis set. For the ground state PEC of Mn_2, the cc-pVQZ basis was also explored. Relativistic effects other than those accounted for in the ECPs were neglected in all calculations.

Basis set extrapolation was done using the cc-pVTZ and cc-pVQZ results on the ground states of Cr_2 and Mn_2. In this process, the total GVVPT2 energy ($E_{tot,GVVPT2}$) was separated into an MCSCF part (E_{MCSCF}) and a dynamic correlation part (E_{dy}). That is,

$$E_{dy} = E_{tot,GVVPT2} - E_{MCSCF} \quad (1)$$

The MCSCF part was extrapolated following the exponential extrapolation scheme originally suggested by Feller for SCF,[86,87] thus

$$E_{\infty,MCSCF} = E_{x,MCSCF} - A\exp(-Bx) \quad (2)$$

where $E_{\infty,MCSCF}$ refers to the expected asymptotic limit of the MCSCF energy at the CBS limit, $E_{x,MCSCF}$ is the calculated MCSCF energy, x is the cardinal number of the basis set (x = 3 for cc-pVTZ, x = 4 for cc-pVQZ), while A and B are fitting parameters. A value of 1.63 for the B parameter has been shown to give good results for SCF extrapolation for many molecules (e.g., see refs 88 and 89). In this work, we tried B = 1.63 and B = 1 (which gave good results in previous GVVPT2/MCSCF studies on NO^-).[90] B = 1.63 performed excellently for Mn_2 but not so well for Cr_2 (see Figures 4 and 8 in the Results and Discussion section). With the value of B defined, a two-point extrapolation expression can easily be obtained from eq 2. The dynamic correlation part of the total energy was extrapolated following the two-point linear fit of Helgaker et al.[91] and of Halkier et al.[92] built upon the ideas of Schwartz,[93] i.e.,

$$E_{\infty,dy} = E_{x,dy} - Cx^{-3} \quad (3)$$

where $E_{\infty,dy}$ is the dynamic correlation energy at the CBS limit, $E_{x,dy}$ is the computed value, with x again being the cardinal number of the basis set, while C is an undetermined parameter.

dx.doi.org/10.1021/jp300401u | J. Phys. Chem. A 2012, 116, 4590−4601

Substituting $x = 3$ for the triple-ζ basis and $x = 4$ for the quadruple-ζ basis set into eq 4 to obtain two equations and then eliminating C results in a two-point extrapolation expression for the dynamic correlation energy. The total energy at the CBS limit is calculated as the sum of the extrapolated static (MCSCF) and dynamic correlation energies

$$E_{\infty,\mathrm{total}} = E_{\infty,\mathrm{MCSCF}} + E_{\infty,\mathrm{dy}} \tag{4}$$

The effective bond order (EBO), $\tilde{n}$, for the ground electronic states of Sc_2, Cr_2, and Mn_2 was determined as

$$\tilde{n} = \frac{\sum_i n_i c_i^2}{\sum_i c_i^2} \tag{5}$$

where n_i is the EBO for each important configuration contributing to the GVVPT2 wave function, and c_i is its corresponding amplitude. For a given configuration, its EBO was determined based on the formula

$$n_i = \frac{1}{2}(n_\mathrm{b} - n_\mathrm{ab}) \tag{6}$$

where n_b and n_ab are the number of bonding and antibonding electrons, respectively.

3. RESULTS AND DISCUSSION

3.1. Sc_2: $X^5\sum_u^-$, $1^3\sum_u^-$, and $1^3\sum_g^-$. The PECs obtained for the lowest quintet state of Sc_2 at the GVVPT2 level of theory and two different active spaces are shown in Figure 1 together

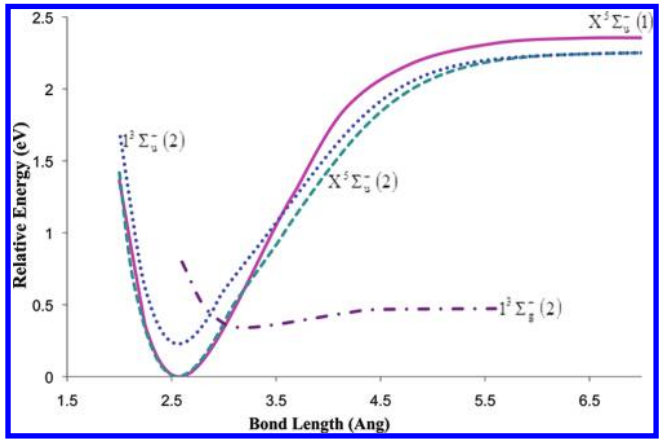

Figure 1. PECs for the $X^5\sum_u^-$, $^3\sum_u^-$ and $^3\sum_g^-$ states of Sc_2 obtained at the GVVPT2 level of theory with the cc-pVTZ basis set. The energies of the two triplet states are plotted relative to the lowest energy value of the quintet ground state obtained from Case 2 partitioning scheme. The numbers 1 or 2 in parentheses after the term symbols in the curve labels denote Case 1 or Case 2 model space.

with the curves for the two triplets also investigated ($1^3\sum_u^-$ and $1^3\sum_g^-$). Corresponding spectroscopic constants characterizing the curves in Figure 1 are displayed in Table 1. In Figure 1, two curves are shown for the quintet state resulting from the different partitioning schemes of the active space (Cases 1 and 2, described above). The two results are similar at short bond lengths, with the only difference being that at long bond lengths, Case 1 partitioning predicts a somewhat higher binding energy (D_e = 2.36 eV versus 2.25 eV). Case 1 partitioning resulted in a model space dimension of only 34 and an overall dimension of approximately 261 million CSFs compared with 610 and about 1.5 billion CSFs, respectively, for Case 2 partitioning. The GVVPT2 part took 28.65 s for Case 1 and 53.42 s for Case 2 reference spaces (on a dual-core AMD Opteron processor 2212 model 65). The leading configuration in both cases was found to be $3d_{xz}\pi_u^1\ 3d_{yz}\pi_u^1\ 4s\sigma_g^2\ 3d_{z^2}\sigma_g^1\ 4s\sigma_u^1$, contributing approximately 0.74 by weight to the total ground electronic state wave function in Case 1 partitioning and about 0.81 by weight in Case 2 partitioning near the minimum (2.57 Å). The EBO for the quintet ground state, determined from the Case 2 reference space using seven important CSFs (the least with an amplitude of 0.101 and the largest with an amplitude of 0.902), was 1.83.

The Case 2 partitioning scheme was used to investigate the triplet excited states. The wave function used to generate the curve shown in Figure 1 for the $^3\sum_u^-$ state was verified to obey the true $D_{\infty h}$ symmetry of the molecule. This curve lies at some 0.23 eV above the quintet ground state and has the same dissociation channel and about the same bond length as does the ground state ($R_e \approx 1.56$ Å). The $^3\sum_g^-$ state, which dissociates to ground state atoms, is van der Waals-like (R_e = 3.19 Å, D_e = 0.13 eV, and ω_e = 114.8 cm^{-1}). The energy gap between the dissociation asymptotes for this state and the quintet ground state was found to be about 1.78 eV, which is 0.35 eV larger than the experimental value of 1.427 eV.

The $^3\sum_u^-$ state competes with $^5\sum_u^-$ for being the ground state, as previous theoretical studies have shown. In this work, the triplet state was found to have two MCSCF solutions at bond lengths ≤3.7 Å: one with broken symmetry (i.e., D_{2h} but not $D_{\infty h}$) and another with proper $D_{\infty h}$ symmetry. At the GVVPT2 level, the former solution was found to be 0.18 eV more stable than the $^5\sum_u^-$ state, whereas the latter solution was 0.23 eV above the $^5\sum_u^-$ state. These results demonstrate once again that calculations should be carefully assessed for symmetry breaking.

3.2. Cr_2: $X^1\sum_g^+$, $^3\sum_u^+$, $^5\sum_g^+$, and $^7\sum_u^+$. The PECs for the singlet ground state of Cr_2 obtained at the MCSCF and GVVPT2 levels of theory are shown in Figures 2 and 3, respectively. The MCSCF curves look similar (irrespective of basis set) and have no resemblance with the experimental curve (e.g., no outer shelf is seen, and all curves predict the ground state to be almost unbound, $D_e \approx 0.12$ eV only). The effect of dynamic electron correlation is profound, as can be seen on comparison of Figures 2 and 3. GVVPT2 adds dynamic correlation energy of about 1.0 hartree to an MCSCF energy of roughly 2086.7 hartree (considering the cc-pVTZ basis set), yet *qualitatively* changes the curves.

Observing Figure 3, it appears that the ECP basis sets investigated (Stuttgart RSC 1997, LANL2DZ, and LANL08) do not satisfactorily describe the bonding in the ground state of Cr_2. This corroborates the recent work that showed ECP basis sets to perform poorly[95] on TM systems in comparison with all-electron basis sets at the DFT level of theory, predicting binding energies with deviations from correct values of up to 5.8 kcal/mol or 0.25 eV (for Sc_2). On the other hand, Dunning-type basis sets (cc-pVTZ, aug-cc-pVTZ, cc-pVQZ) do well, reproducing essential characteristics of the RKR experimental curve. The spectroscopic constants characterizing these curves are given in Table 2. The best results are obtained with cc-pVQZ (R_e = 1.80 Å compared with an experimental value of 1.68 Å[49] and D_e = 1.47 eV compared with an experimental value of 1.47 ± 0.056[51]) and with aug-cc-pVTZ (ω_e = 412.6 cm^{-1} compared with an experimental value of 481 cm^{-1}).[53] Near the minimum (1.84 Å), the leading configuration in the GVVPT2 wave function for the Cr_2 ground state was

dx.doi.org/10.1021/jp300401u | J. Phys. Chem. A 2012, 116, 4590−4601

Table 1. Equilibrium Distances (R_e), Binding Energies (D_e), and Harmonic Frequencies (ω_e) of three Electronic States of Sc_2 Calculated at the GVVPT2 Level of Theory Compared with Results by Other Methods

electronic state	method	basis set	R_e (Å)	D_e (eV)	ω_e (cm^{-1})
$X^5\sum_u^-$					
	MRCI + Q[a]	cc-pV5Z	2.75	2.17	224.0
	PC-NEVPT2[b]	(21s15p10d6f4g2h)	2.58	1.74	257.5
	GVVPT2[c]	cc-pVTZ	2.57	2.36	255.9
	GVVPT2[d]	cc-pVTZ	2.57	2.25	258.1
	experiment				238.9[e]
$1^3\sum_u^-$					
	MRCI + Q[a]	cc-pV5Z	2.74	2.13	234.0
	PC-NEVPT2[b]	(21s15p10d6f4g2h)	2.60	1.65	260.1
	GVVPT2[f]	cc-pVTZ	2.57	2.03	264.0
	GVVPT2[g]	cc-pVTZ	2.60	2.44	503.8
$1^3\sum_g^-$					
	MRCI + Q[a]	cc-pV5Z	3.45	0.23	93.4
	GVVPT2[d]	cc-pVTZ	3.19	0.13	114.8

[a]Reference 11. [b]Reference 15. [c]This work (Case 1). [d]This work (Case 2). [e]Reference 20. [f]This work (Case 2, proper symmetry solution). [g]This work (Case 2, broken symmetry solution).

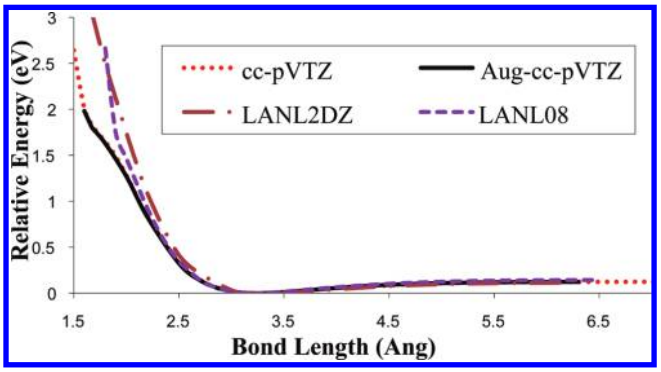

Figure 2. PECs for the singlet ground electronic state, $X^1\sum_g^+$, of Cr_2 obtained at the MCSCF level of theory using the basis sets indicated in the inset.

$3d_{xz}\pi_u^2\ 3d_{yz}\pi_u^2\ 3d_{z^2}\sigma_g^2\ 3d_{x^2-y^2}\ \delta_g^2\ 3d_{xy}\delta_g^2 4s\sigma_g^2$ with an amplitude of 0.401. Three other important configurations were $3d_{xz}\pi_u^2 3d_{yz}\pi_u^2 3d_{z^2}\sigma_g^2 3d_{x^2-y^2}\delta_g^1 3d_{x^2-y^2}\delta^{*1}_u 3d_{xy}\delta_g^1 3d_{xy}\delta^{*1}_u 4s\sigma_g^2$, and $3d_{xz}\pi_u^2 3d_{yz}\pi_u^2 3d_{z^2}\sigma_g^2 3d_{x^2-y^2}\delta_g^2 3d_{xy}\delta^{*2}_u 4s\sigma_g^2$ with amplitudes of 0.237, 0.235 and 0.235, respectively. Using 22 CSFs with

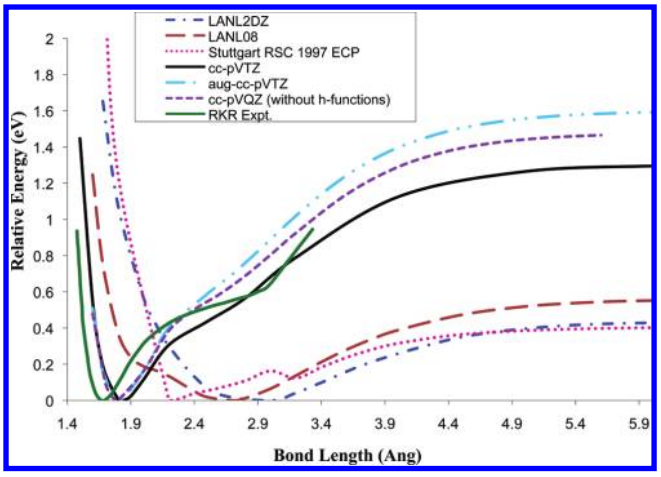

Figure 3. PECs for the singlet ground state, $X^1\sum_g^+$, of Cr_2 obtained at the GVVPT2 level of theory with different basis sets as indicated in the inset.

Table 2. Basis Set Effect on the Equilibrium Bond Length, R_e (Å), Dissociation Energy, D_e (eV), and the Harmonic Frequency, ω_e (cm^{-1}) for Cr_2 in Its Ground State, $X^1\sum_g^+$

	GVVPT2			MCSCF	
basis set	R_e	D_e	ω_e	R_e	D_e
cc-pVTZ	1.83	1.30	346.4	3.30	0.12
aug-cc-pVTZ	1.81	1.60	412.6	3.30	0.12
cc-pVQZ	1.80	1.47	364.4		
LANL2DZ	3.00	0.56		3.40	0.11
LANL08	2.70	0.43		3.20	0.14
Stuttgart RSC 1997 ECP	2.22	0.41			
experiment	1.68[a]	1.472 ± 0.056[b] 1.56 ± 0.06[c] 1.45 ± 0.1[d]	481[e]		

[a]Reference 49. [b]Reference 51. [c]Reference 50. [d]Reference 52. [e]Reference 53.

amplitudes in the range [0.0811, 0.4011], we obtained an EBO of 4.37 (compared with 4.51 at the CASPT2 level[96,97]). The amplitudes of these configurations decrease toward the shelf region so that, at 2.80 Å, the amplitude of the first configuration is only 0.082 (with cc-pVTZ basis). Using 119 CSFs at 2.8 Å with amplitudes in the range [0.0581, 0.0902] gave an EBO of only 1.37.

The results of the extrapolation of the ground state PEC of Cr_2 to the CBS limit (using the cc-pVTZ and cc-pVQZ results) are shown in Figure 4. Extrapolation of the MCSCF part of the total energy using $B = 1$ in eq 3 resulted in a PEC virtually the same as the cc-pVQZ curve at all geometries, while using $B = 1.63$ led to a slight decrease in bond length from 1.80 Å for cc-pVQZ to 1.78 Å at CBS. With $B = 1.63$, the binding energy was overestimated by some 0.30 eV.

Finally, we investigated the lowest triplet ($^3\sum_u^+$), quintet ($^5\sum_g^+$), and septet ($^7\sum_u^+$) excited states of Cr_2 at the GVVPT2 level of theory using the cc-pVTZ basis set. The PECs for these states are shown in Figure 5 together with the ground state and RKR experimental curves. The spectroscopic constants characterizing the curves for the excited electronic states of Cr_2 are shown in Table 3 and compared with the CASPT2 results obtained by Andersson.[98]

dx.doi.org/10.1021/jp300401u | J. Phys. Chem. A 2012, 116, 4590−4601

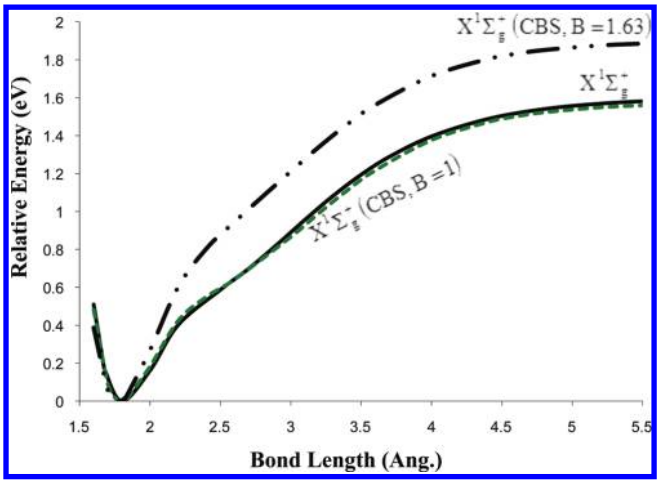

Figure 4. Basis set extrapolation on the $X^1\sum_g^+$ state PEC of Cr_2 with different values of the B parameter in eq 2 as indicated in the labels for the curves.

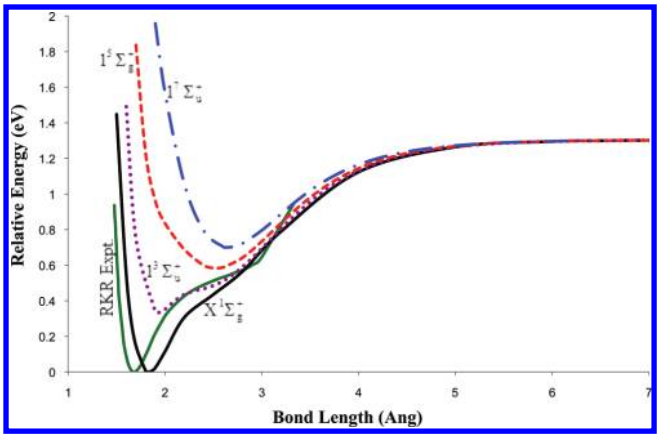

Figure 5. PECs for the $X^1\sum_g^+$, lowest $^3\sum_u^+$, $^5\sum_g^+$, and $^7\sum_u^+$ states of Cr_2 obtained at the GVVPT2 level of theory with the cc-pVTZ basis set. All energies for computed states are plotted relative to the lowest energy value of the lowest lying curve (the singlet ground state).

Table 3. Spectroscopic Constants for Excited Electronic States of Cr_2 Obtained at the GVVPT2 Level with the cc-pVTZ Basis Set Compared with Those of Ref 98 Calculated at the CASPT2 Level of Theory

	GVVPT2				CASPT2[a]		
electronic state	R_e (Å)	D_e (eV)	ω_e (cm^{-1})	T_e (eV)	R_e (Å)	ω_e (cm^{-1})	T_e (eV)
$1\ ^3\sum_u^+$	1.93	0.97	307.0	0.33	1.86	410	0.56
$1\ ^5\sum_g^+$	2.53	0.72	140.9	0.58	2.58	148	0.78
$1\ ^7\sum_u^+$	2.65	0.60	155.9	0.70	2.67		0.88

[a]Reference 98.

3.3. Mn_2: $X^1\sum_g^+, {}^5\sum_g^+, {}^9\sum_g^+$. The PECs obtained at the GVVPT2 level for the electronic states of Mn_2 are shown in Figures 6−8 for Cases A−D. It can be seen that the results depend fairly strongly on the nature of partitioning of the active space. Case A partitioning (where the four sigma MOs derived from $3d_z^2$ and 4s were grouped together in one valence subspace in order to allow for some bonding involving the 4s-dominated MOs), when used to investigate the singlet ground state gave a bond length that was incorrect (R_e = 4.58 Å compared with the experimental value of 3.40 Å), although a binding energy of D_e = 0.069 eV was quite good. This reference model space (Case A) was not used to investigate excited states due to this rather poor R_e value. Case B partitioning was derived from Case A by further increasing the active space within the 3d/4s manifold (by grouping the four 3d-derived π orbitals in one valence subspace), and yielded a PEC with good characteristics for the singlet ground state. The spectroscopic constants of R_e = 3.37 Å, D_e = 0.11 eV, and ω_e = 83.35 cm^{-1} obtained with Case B model space are close to the experimental values of 3.40 Å, 0.10 eV, and 68.1 cm^{-1}, respectively (see Figure 6 and Table 4). Unfortunately with this partitioning, the

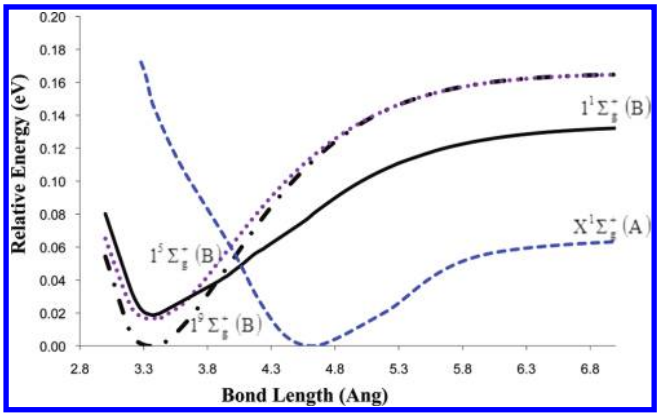

Figure 6. PECs for the $X^1\sum_g^+$, and lowest $^5\sum_g^+$, and $^9\sum_g^+$ states of Mn_2 obtained at the GVVPT2 level of theory with the cc-pVTZ basis set. All energies from Case B calculations are plotted relative to the lowest energy value of the lowest lying curve (the nonet state). Letters A or B in parentheses after the term symbols in the curve labels denote Case A or B partitioning scheme of the reference space.

quintet, $^5\sum_g^+$, and nonet, $^9\sum_g^+$, excited electronic states that should have the same dissociation channel as the singlet ground state do not (cf. Figure 6). Moreover, these excited states appear to be slightly more stable (i.e., 0.02 eV) than the ground state in the vicinity of the equilibrium bond length. Yet, our analysis of the orbitals did not reveal significant changes in their nature for any of the three electronic states. We conclude that this active space (Case B) is again insufficient for describing the Mn_2 system. Detailed orbital analysis indicated that the sixth b_{1u} MO in D_{2h} symmetry (expected to be 4s-dominated) was exchanged with the fifth b_{1u} MO ($3p_z$-dominated). This observation supports the argument of Camacho et al.[31] that the $3p_z$-derived antibonding MO is important for an adequate description of the bonding in ground state Mn_2. Therefore, we included the $3p_z$-dominated antibonding MO (and also its bonding counterpart in order to permit good dissociation into equivalent fragments) into the sigma subspace of Case B to obtain the reference model space labeled Case C.

The PECs for the three electronic states obtained with the Case C active space of 14 MOs and 18 electrons (14, 18) at the GVVPT2 level using the cc-pVTZ basis set are shown in Figure 7. All three states have $R_e \approx 4.10$ Å, but rather than have the same dissociation asymptote, as should be the case, the quintet and nonet states (which appear to be quasidegenerate) are separated from the singlet ground state by about 0.015 eV at a bond length of 16.0 Å. Difficulties in describing the bonding in Mn_2 when involving the 4s-derived MOs in the active space were first observed by Yamamoto et al.[32] Without state averaging, these authors obtained three kinds of CASSCF solutions at intermediate bond lengths, which did not permit

dx.doi.org/10.1021/jp300401u | J. Phys. Chem. A 2012, 116, 4590−4601

Table 4. Equilibrium Distances (R_e), Binding Energies (D_e), and Harmonic Frequencies (ω_e) of Three Electronic States of Mn_2 Calculated at the GVVPT2 Level of Theory Compared with Results from Other Methods

electronic state	method	basis set	R_e (Å)	D_e (eV)	ω_e (cm^{-1})
$X^1\sum_g^+$	MRCI[a]	aug-cc-pVQZ	4.13	0.03	24.3
	MRCI + Q[a]	aug-cc-pVQZ	3.80	0.05	36
	ACPF[a]	aug-cc-pVQZ	3.64	0.06	42
	CASPT2[b]	ANO-RCC 6s5p4d3f2g1h	3.19	0.28	
	NEVPT2/SC + s[c]	ANO-RCC 6s5p4d3f2g1h	3.70	0.08	
	GVVPT2[d]	cc-pVTZ	3.37	0.11	83.4
	GVVPT2[e]	cc-pVQZ	3.83	0.05	30.7
	experiment		3.40[f]	0.02−0.15[g]	68.1[h]
$^5\sum_g^+$					
	MRCI[a]	aug-cc-pVQZ	4.13	0.03	24.6
	MRCI + Q[a]	aug-cc-pVQZ	3.81	0.05	34
	ACPF[a]	aug-cc-pVQZ	3.67	0.06	41
	CASPT2[b]	ANO-RCC 6s5p4d3f2g1h	3.23	0.27	
	GVVPT2[d]	cc-pVTZ	4.09	0.04	26.4
$^9\sum_g^+$					
	MRCI[a]	aug-cc-pVQZ	4.14	0.03	24.5
	MRCI + Q[a]	aug-cc-pVQZ	3.84	0.05	35
	ACPF[a]	aug-cc-pVQZ	3.72	0.05	38
	CASPT2[b]	ANO-RCC 6s5p4d3f2g1h	3.30	0.25	
	AQCC/LC[c]	AV5Z	3.85	0.04	
	GVVPT2[d]	cc-pVTZ	4.08	0.04	27.0

[a]Reference 8. [b]Reference 5. [c]Reference 26. (SC + s designation implies that all 3s3p3d4s electrons were correlated, SC stands for "small core"). [d]This work (Case B). [e]This work (Case D). [f]Reference 7. [g]Reference 30. [h]Reference 25.

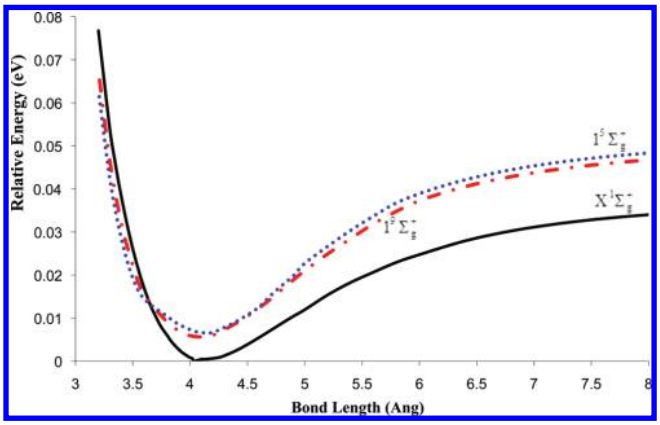

Figure 7. PECs for the $X^1\sum_g^+$, lowest $^5\sum_g^+$, and $^9\sum_g^+$ states of Mn_2 obtained at the GVVPT2 level of theory and Case C model space with the cc-pVTZ basis set. All energies are plotted relative to the lowest energy value of the lowest lying curve (the singlet ground state).

the construction of a smooth PEC at the second-order multiconfigurational quasidegenerate perturbation theory (MCQDPT2) level of theory. This problem of discontinuities in the Mn_2 PEC due to multiple CASSCF (or MCSCF) solutions, rather than intruder state problems, was also observed by Camacho et al.[31] in their multireference Møller−Plesset perturbation theory (MRMP) study. In our calculations with Case C model space, when beginning from long bond lengths and gradually decreasing the Mn−Mn bond, we observed a sharp discontinuity in the MCSCF energy between 4.4 and 4.3 Å for all three electronic states investigated. However, when we resumed calculations with the lower energy orbitals as our initial orbitals at the points where the discontinuities were observed (i.e., performing single point energy calculations inward to shorter bond lengths and outward to longer bond lengths), no discontinuities were observed, and the smooth curves reported in Figure 7 were constructed. State averaging was not necessary at the MCSCF level for convergence.

Our analysis of the important CSFs contributing to the wave functions for the studied electronic states revealed that the $3p_z$- and 4s-derived MOs were doubly occupied in all dominant CSFs, implying inactivity. In retrospect, it is not surprising that the 4s orbitals do not seem to play an important role in the bonding in Mn_2. The large difference between the average radii of the 3d and 4s subshells of the Mn atom (1.13 vs 3.38 b)[99] indicates that their spatial extents are quite different and, as in dichromium, these orbitals cannot simultaneously contribute to bonding at the same internuclear distance. However, no outer shelf is observed in contrast to the situation in Cr_2. Whereas there is strong bonding in Cr_2, there is only weak van der Waals-like interaction (i.e., weak binding, D_e = 0.1 eV only, and long internuclear distance of 3.4 Å)[8] in Mn_2 that has been ascribed to the shielding effect of the doubly occupied 4s orbitals on the 3d subshells.

The results of the fourth tested reference model space (Case D) are shown in Figure 8 and Table 4. With the $3p_z$- and 4s-derived MOs moved from the active space into the active core, the $X^1\sum_g^+$, $^5\sum_g^+$, and $^9\sum_g^+$ states are all degenerate with $R_e \approx$ 4.09 Å, D_e = 0.04 eV, and $\omega_e \approx 27$ cm^{-1} using the cc-pVTZ basis set. Analysis of the configuration structure of these states' wave functions did not show any dominant electron configurations. For the ground electronic state, we used 132 CSFs at 4.08 Å with amplitudes in the range [0.0698, 0.0944] and obtained an EBO of only 0.01. The ground state PEC with cc-pVQZ has a somewhat shorter bond length (R_e = 3.83 Å), higher binding energy (D_e = 0.05 eV) and harmonic frequency (ω_e = 30.7 cm^{-1}).

Extrapolation of the ground state PEC to the CBS limit, using B = 1.63 in eq 2, gives R_e = 3.40 Å and D_e = 0.09 eV, which are in very good agreement with experiment. However,

dx.doi.org/10.1021/jp300401u | J. Phys. Chem. A 2012, 116, 4590−4601

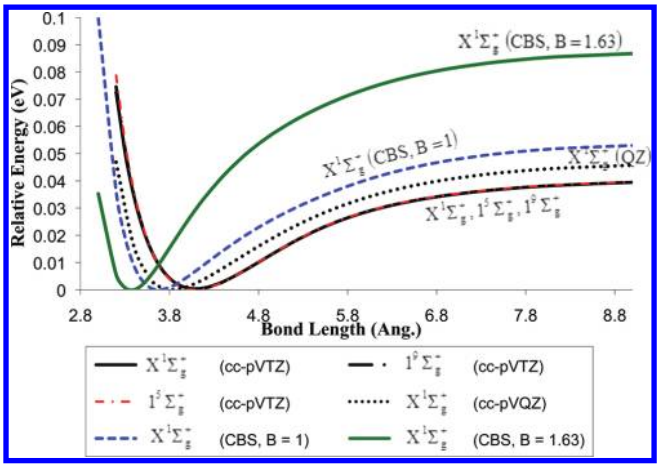

Figure 8. PECs for the $X^1\sum_g^+$, $^5\sum_g^+$, and $^9\sum_g^+$ states of Mn_2 obtained at the GVVPT2 level of theory and Case D model space with the cc-pVTZ basis set and then cc-pVQZ + extrapolation to the CBS limit for the singlet ground state only. All energies for the three states computed with cc-pVTZ are plotted relative to the lowest energy value of the lowest lying curve (the singlet ground state).

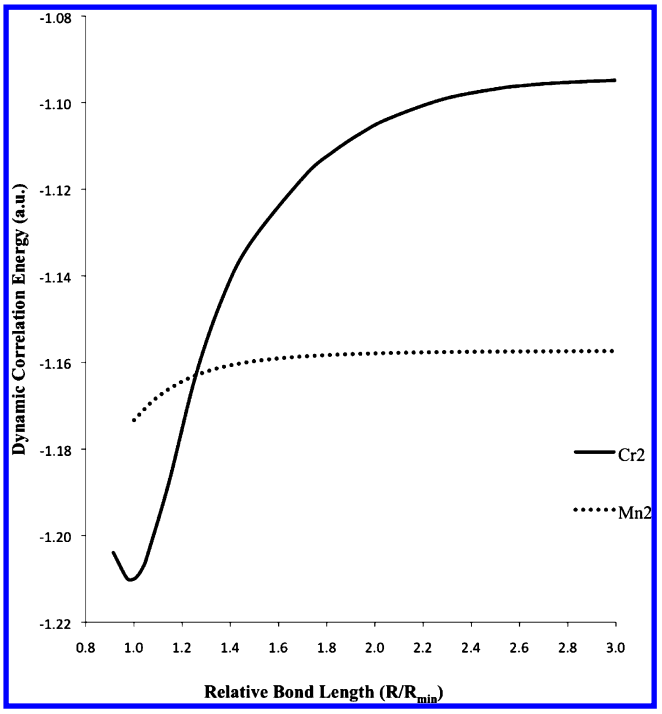

Figure 9. Variation of dynamic correlation energy as a function of relative bond length (R/R_{min}) for diatomic Cr and Mn. R_{min} is the bond length at which the dynamic correlation energy is a minimum.

when $B = 1$ is used, which proved efficacious for Cr_2 as it did in previous GVVPT2/MCSCF studies,[90] the results were only slightly improved (e.g., $R_e = 3.7$ Å and $D_e = 0.06$ eV) from the cc-pVQZ values. Although a detailed analysis of extrapolation of GVVPT2/MCSCF is outside the scope of the present work, additional insight can be gained by a closer examination of the variation in correlation energy with geometry between Cr_2 and Mn_2. Although neither the full CI curves nor restricted HF curves are available for Cr_2 and Mn_2, because of computational expense and complete failure of a single determinant function, respectively, and consequently a partitioning of total correlation energy into nondynamic and dynamic contributions cannot be made, it is possible to plot the dynamic correlation energy from GVVPT2 calculations as a function of internuclear distance (cf. Figure 9). It can be seen that the dynamic correlation energy recovered by GVVPT2 is almost independent of bond length for Mn_2 but varies significantly with changing bond length for Cr_2. Recognizing that correlation is not cleanly divided into dynamic and nondynamic contributions, and that MCSCF includes some correlation that might be more appropriately considered dynamic than nondyanmic, Figure 9 supports the supposition that Cr_2 has significantly greater variation in nondynamic correlation than does Mn_2. Considering that eq 2, describing CBS extrapolation for nondynamic correlation, was initially developed for extrapolation of HF energies[86,87] and that one should expect HF-type extrapolation to work best if the fraction of correlation energy within the MCSCF function is roughly independent of internuclear distance, one should expect that eq 2 will be more efficacious for Mn_2 and that the constant developed for HF ($B = 1.63$) is more likely to be reasonable.

The model space

$$(3d_{xz}\pi_u 3d_{xz}\pi_g^*)^2(3d_{yz}\pi_u 3d_{yz}\pi_g^*)^2(3d_{z^2}\sigma_g 3d_{z^2}\sigma_u^*)^2$$
$$(3d_{x^2-y^2}\delta_g 3d_{x^2-y^2}\delta_u^*)^2(3d_{xy}\delta_g 3d_{xy}\delta_u^*)^2$$

called Case D, proved to be the best active space for this molecule. It seems that inclusion of the $3p_z$- and/or 4s-derived MOs into the active space for Mn_2 creates more problems than it solves. Exploratory calculations on the first excited state of $^1\sum_g^+$ symmetry showed that active core excitations were not significant; consequently, inclusion of the $3p_z$- and 4s-derived MOs in the active core also does not appear to compromise the description of the lowest-lying excited state. In Case D calculations, no discontinuities whatsoever, due to multiple MCSCF solutions, were observed at any geometry. Our somewhat long bond lengths (both for Cr_2 and Mn_2) may be due to our choice of a simple zero-order Hamiltonian, neglect of scalar relativistic effects, and possibly that the highest angular momentum functions that we could use were *g* functions (i.e., $l = 4$; N.B. for calculations with cc-pVQZ, the h-functions were neglected).

4. CONCLUSIONS

The GVVPT2 method was shown to be capable of describing complicated ground and low-lying excited electronic states of first-row TM dimers, using chemically intuitive valence orbitals. Even when using a simple zero-order Hamiltonian and ignoring scalar relativistic effects, we have shown that the GVVPT2 method gives PECs and spectroscopic constants that are close to experimental results using triple split valence basis sets and model spaces derived from valence bond models. Particularly noteworthy is the fact that the curves, in addition to being smooth and continuous, are free of artifactual inflections for both ground and excited states.

This study revealed that a proper description of several of the low-lying electronic states of Cr_2 can be made using a simple model space consisting of only 3d and 4s-derived MOs, resulting in model space dimensions of 1516, 2712, and 580 CSFs, and total space dimensions of 998 024 048, 2 141 100 436, and 920 000 422 CSFs for the $X^1\sum_g^+$, $1^3\sum_u^+$, and $1^7\sum_u^+$ electronic states, respectively, using the cc-pVTZ basis set. It was observed that both valence double-ζ and valence triple-ζ ECP basis sets perform poorly for Cr_2.

dx.doi.org/10.1021/jp300401u | J. Phys. Chem. A 2012, 116, 4590−4601

Our calculations support the generally held view that the ground state of Sc_2 is $1^5\sum_u^-$. Spectroscopic constants are in quite good agreement with MRCISD+Q/cc-pV5Z and experimental results. Notably, D_e at the MRCISD+Q/cc-pV5Z[11] is 2.17 eV, while GVVPT2/cc-pVTZ obtains 2.25 eV; experiment[20] obtained 239 cm^{-1} for ω_e, with MRCISD+Q/cc-pV5Z being 15 cm^{-1} lower and GVVPT2/cc-pVTZ being 19 cm^{-1} higher.

Studies of Mn_2 emphasized the importance of selecting the right set of MOs to define the active space and properly partitioning these MOs to give reference macroconfigurations. Including either $3p_z$- or 4s-derived MOs into the active space for Mn_2 unnecessarily increased the dimension of the active space and, more importantly, introduced multiple MCSCF solutions at certain geometries. Moreover, obtaining correct dissociation degeneracies required the use of proper reference spaces. A good description of the interaction of Mn atoms in Mn_2 can be achieved with an active space of 10 3d-derived MOs with 10 active electrons while correlating the 3s, 3p and 4s electrons at the GVVPT2 level of theory.

In all, by following reference spaces derived from, but generally not identical to, simple valence bond models, the GVVPT2 method does a good job in describing the bonding in ground state Sc, Cr, and Mn diatomic molecules and their low-lying excited electronic states. This study has significantly extended the range of problems that GVVPT2 has been shown to address well. And, perhaps more significantly, it has shown that unusual active spaces (e.g., involving orbitals that would not be expected from chemical principles) do not need to be included to reasonably describe both ground and low-lying excited electronic states of TM molecules that have previously been considered to be problematic.

AUTHOR INFORMATION

Corresponding Author

*E-mail: mhoffmann@chem.und.edu. Phone: +1-701-777-2742.

Notes

The authors declare no competing financial interest.

ACKNOWLEDGMENTS

The authors are grateful to the National Science Foundation (Grant No. EPS-0814442) for financial support.

REFERENCES

(1) Oymak, H.; Erkoç, S. *Phys. Rev. A.* **2002**, *66*, 033202/1−10.
(2) Demangeat, C.; Parbelas, J. C. *Rep. Prog. Phys.* **2002**, *65*, 1679−1739.
(3) Lombardi, J. R.; Davis, B. *Chem. Rev.* **2002**, *102*, 2431−2460.
(4) Cheeseman, M.; Van Zee, R. J.; Flanagan, H. L.; Weltner, W., Jr. *J. Chem. Phys.* **1990**, *92*, 1553−1559.
(5) Negodaev, I.; de Graaf, C.; Caballol, R. *Chem. Phys. Lett.* **2008**, *458*, 290−294.
(6) Gu, J. H.; Zhu, Z. L. *Acta Metall. Sin. (Engl. Lett.)* **2007**, *20*, 341−346.
(7) Baumann, C. A.; Van Zee, R. J.; Bhat, S. V.; Weltner, W., Jr. *J. Chem. Phys.* **1983**, *78*, 190−199.
(8) Tzeli, D.; Miranda, U.; Kaplan, I. G.; Mavridis, A. *J. Chem. Phys.* **2008**, *129*, 154310/1−8.
(9) Camacho, C.; Witek, H. A.; Yamamoto, S. *J. Comput. Chem.* **2009**, *30*, 468−478.
(10) Langhoff, S. R.; Bauschlicher, C. W., Jr. *Annu. Rev. Phys. Chem.* **1988**, *39*, 181−212.
(11) Kalemos, A.; Kaplan, I. G.; Mavridis, A. *J. Chem. Phys.* **2010**, *132*, 024309/1−7.
(12) Yamanaka, S.; Ukai, T.; Nakata, K.; Takeda, R.; Shoji, M.; Kawakami, T.; Takada, T.; Yamaguchi, K. *Int. J. Quantum Chem.* **2007**, *107*, 3178−3190.
(13) Edgecombe, K. E.; Becke, A. D. *Chem. Phys. Lett.* **1995**, *244*, 427−432.
(14) Thomas, E. J., III; Murray, J. S.; O'Connor, C. J.; Politzer, P. *J. Mol. Struct.* **1999**, *487*, 177−182.
(15) Camacho, C.; Witek, H. A.; Cimiraglia, R. *J. Chem. Phys.* **2010**, *132*, 244306/1−9.
(16) Khait, Y. G.; Song, J.; Hoffmann, M. R. *J. Chem. Phys.* **2002**, *117*, 4133−4145.
(17) Jiang, W.; Khait, Y. G.; Hoffmann, M. R. *J. Chem. Phys. A* **2009**, *113*, 4374−4380.
(18) Knight, L. B.; Van Zee, J. R.; Weltner, W. *Chem. Phys. Lett.* **1983**, *94*, 296−299.
(19) Singer, R. J.; Grinter, R. *Chem. Phys.* **1987**, *113*, 99−109.
(20) Moskovits, M.; Lella, D. P.; Limm, W. *J. Chem. Phys.* **1984**, *80*, 626−633.
(21) Verhaegen, G.; Smoes, S.; Drowart, J. *J. Chem. Phys.* **1964**, *40*, 239−241.
(22) Matxain, J. M.; Rezabal, E.; Lopez, X.; Ugalde, J. M.; Gagliardi, L. *J. Chem. Phys.* **2008**, *128*, 194315/1−5.
(23) Matxain, J. M.; Rezabal, E.; Lopez, X.; Ugalde, J. M.; Gagliardi, L. *J. Chem. Phys.* **2010**, *132*, 139901/1.
(24) Kaplan, I. G.; Miranda, U. *AIP Adv.* **2011**, *1*, 022108/1−9.
(25) Kirkwood, A. D.; Bier, K. D.; Thompson, J. K.; Haslett, T. L.; Huber, A. S.; Moskovits, M. *J. Phys. Chem.* **1991**, *95*, 2644−2652.
(26) Buchachenko, A. A.; Chalasinski, G.; Szczęśniak, M. M. *J. Chem. Phys.* **2010**, *132*, 024312/1−9.
(27) Van Zee, R. J.; Baumann, C. A.; Weltner, W., Jr. *J. Chem. Phys.* **1981**, *74*, 6977−6978.
(28) Cheeseman, M.; Van Zee, R. J.; Weltner, W., Jr. *J. Chem. Phys.* **1989**, *91*, 2748−2749.
(29) Bier, K. D.; Haslett, T. L.; Kirkwood, A. D.; Moskovits, M. J. *J. Chem. Phys.* **1988**, *89*, 6−12.
(30) Haslett, T. L.; Moskovits, M.; Weitzman, A. L. *J. Mol. Spectrosc.* **1988**, *135*, 259−269.
(31) Camacho, C.; Yamamoto, S.; Witek, H. A. *Phys. Chem. Chem. Phys.* **2008**, *10*, 5128−5134.
(32) Yamamoto, S.; Tatewaki, H.; Moriyama, H.; Nakano, H. *J. Chem. Phys.* **2006**, *124*, 124302/1−8.
(33) Koga, T.; Tatewaki, H.; Matsuyama, H.; Satoh, Y. *Theor. Chem. Acc.* **1999**, *102*, 105−111.
(34) Tatewaki, H.; Koga, T.; Yamamoto, S. *Theor. Chem. Acc.* **2000**, *105*, 55−61.
(35) Sekiya, M.; Noro, T.; Osanai, Y.; Koga, T. *Theor. Chem. Acc.* **2001**, *106*, 297−300.
(36) Roos, B. O.; Lindh, R.; Malmqvist, P. A.; Veryazov, V.; Widmark, P. O. *J. Phys. Chem. A* **2005**, *109*, 6575−6579.
(37) Angeli, C.; Cavallini, A.; Cimiraglia, R. *J. Chem. Phys.* **2008**, *128*, 244317/1−6.
(38) Nayak, S. K.; Jena, P. *Chem. Phys. Lett.* **1998**, *289*, 473−479.
(39) Briere, T. M.; Sluiter, M. H. F.; Kumar, V.; Kawazoe, Y. *Phys. Rev. B* **2002**, *66*, 064412/1−6.
(40) Jellinek, J.; Acioli, P. H.; Garcia-Rodeja, J.; Zheng, W.; Thomas, O. C.; Bowen, K. H., Jr. *Phys. Rev. B* **2006**, *74*, 153401/1−4.
(41) Bobadova-Parvanova, P.; Jackson, K. A.; Srinivas, S.; Horoi, M. *J. Chem. Phys.* **2005**, *122*, 014310/1−11.
(42) Yamanaka, S.; Ukai, T.; Nakata, K.; Takeda, R.; Shoji, M.; Kawakami, T.; Takada, T.; Yamaguchi, K. *J. Quantum Chem.* **2007**, *107*, 3178−3190.
(43) Kabir, M.; Mookerjee, A.; Kanhere, D. G. *Phys. Rev. B* **2006**, *73*, 224439/1−11.
(44) Kant, A.; Strauss, B. J. *J. Chem. Phys.* **1966**, *45*, 3161−3162.
(45) Kündig, E. P.; Moskovits, M.; Ozin, G. A. *Nature* **1975**, *254*, 503−504.
(46) Salahub, D. R. *Adv. Chem. Phys.* **1987**, *69*, 447−520.

(47) Bauschlicher, C. W., Jr.; Patridge, H. *Chem. Phys. Lett.* **1994**, *231*, 277−282.
(48) Michalopoulos, D. L.; Geusic, M. E.; Hansen, S. G.; Powers, D. E.; Smalley, R. E. *J. Phys. Chem.* **1982**, *86*, 3914−3916.
(49) Bondybey, V. E.; English, J. H. *Chem. Phys. Lett.* **1983**, *94*, 443−447.
(50) Simard, B.; Lebeault-Dorget, M.-A.; Marijnissen, A.; ter Meulen, J. *J. Chem. Phys.* **1998**, *108*, 9668−9674.
(51) Hilpert, K.; Ruthardt, K. *Ber. Bunsen-Ges. Phys. Chem.* **1987**, *91*, 724−731.
(52) Su, C. X.; Hales, D. A.; Armentrout, P. B. *Chem. Phys. Lett.* **1993**, *201*, 199−204.
(53) Casey, S. M.; Leopold, D. G. *J. Phys. Chem.* **1993**, *97*, 816−830.
(54) Rydberg, R. *Z. Phys.* **1931**, *73*, 376−385.
(55) Klein, O. *Z. Phys.* **1932**, *76*, 226−235.
(56) Rees, A. L. G. *Proc. Phys. Soc.* **1947**, *59*, 998−1008.
(57) Scuseria, G. E.; Schaefer, H. F., III. *Chem. Phys. Lett.* **1990**, *174*, 501−503.
(58) Mitrushenkov, A. O.; Palmieri, P. *Chem. Phys. Lett.* **1997**, *278*, 285−290.
(59) Dachsel, H.; Harrison, R. J.; Dixon, D. A. *J. Phys. Chem. A* **1999**, *103*, 152−155.
(60) Andersson, K.; Roos, B. O.; Malmqvist, P. A.; Widmark, P. O. *Chem. Phys. Lett.* **1994**, *230*, 391−397.
(61) Andersson, K.; Roos, B. O. *Chem. Phys. Lett.* **1995**, *245*, 215−223.
(62) Roos, B. O. *Collect. Czech. Chem. Commun.* **2003**, *68*, 265−274.
(63) Andersson, K. *Theor. Chim. Acta* **1995**, *91*, 31−46.
(64) Celani, P.; Stoll, H.; Werner, H. J.; Knowles, P. J. *Mol. Phys.* **2004**, *102*, 2369−2379.
(65) Müller, T. *J. Phys. Chem. A* **2009**, *113*, 12729−12740.
(66) Hess, B. A. *Phys. Rev.* **1986**, *A33*, 3742−3748.
(67) Hess, B. A.; Jansen, G. *Phys. Rev.* **1989**, *A39*, 6016−6017.
(68) Hongo, K.; Maezono, R. *Int. J. Quantum Chem.* **2011**, *00*, 000−000.
(69) Ruipérez, F.; Aquilante, F.; Ugalde, J. M.; Infante, I. *J. Chem. Theory Comput.* **2011**, *7*, 1640−1646.
(70) Kurashige, Y.; Yanai, T. *J. Chem. Phys.* **2011**, *135*, 094104/1−9.
(71) Devarajan, A.; Gaenko, A. V.; Khait, Y. G.; Hoffmann, M. R. *J. Phys. Chem. A* **2008**, *112*, 2677−2682.
(72) Theis, D.; Khait, Y. G.; Pal, S.; Hoffmann, M. R. *Chem. Phys. Lett.* **2010**, *487*, 116−121.
(73) Theis, D.; Khait, Y. G.; Hoffmann, M. R. *J. Chem. Phys.* **2011**, *135*, 044117/1−14.
(74) Mbote, Y. E.; Khait, Y. G.; Hardel, C.; Hoffmann, M. R. *J. Phys. Chem. A* **2010**, *114*, 8831−8836.
(75) Hoffmann, M. R.; Datta, D.; Das, S.; Mukherjee, D.; Szabados, Á.; Rolik, Z.; Surján, P. R. *J. Chem. Phys.* **2009**, *131*, 204104/1−11.
(76) Angeli, C.; Pastore, M.; Cimiraglia, R. *Theor. Chem. Acc.* **2007**, *117*, 743−754.
(77) Dyall, K. G. *J. Chem. Phys.* **1995**, *102*, 4909−4919.
(78) Khait, Y. G.; Song, J.; Hoffmann, M. R. *Int. J. Quantum Chem.* **2004**, *99*, 210−220.
(79) Balabanov, N. B.; Peterson, K. A. *J. Chem. Phys.* **2005**, *123*, 064107/1−15.
(80) Bergner, A.; Dolg, M.; Kuechle, W.; Stoll, H.; Preuss, H. *Mol. Phys.* **1993**, *80*, 1431−1441.
(81) Kaupp, M.; Schleyer, P. R.; Stoll, H.; Preuss, H. *J. Chem. Phys.* **1991**, *94*, 1360−1366.
(82) Dolg, M.; Stoll, H.; Preuss, H.; Pitzer, R. M. *J. Phys. Chem.* **1993**, *97*, 5852−5859.
(83) Hay, P. J.; Wadt, W. R. *J. Chem. Phys.* **1985**, *82*, 270−283.
(84) Hay, P. J.; Wadt, W. R. *J. Chem. Phys.* **1985**, *82*, 284−298.
(85) Roy, L. E.; Hay, P. J.; Martin, R. L. *J. Chem. Theory Comput.* **2008**, *4*, 1029−1031.
(86) Feller, D. *J. Chem. Phys.* **1993**, *98*, 7059−7071.
(87) Feller, D. *J. Chem. Phys.* **1992**, *96*, 6104−6114.
(88) Halkier, A.; Helgaker, T.; Jørgensen, P.; Klopper, W.; Olsen, J. *Chem. Phys. Lett.* **1999**, *302*, 437−446.
(89) Williams, T. G.; De Yonker, N. J.; Wilson, A. K. *J. Chem. Phys.* **2008**, *128*, 044101/1−9.
(90) Jiang, W.; Khait, Y. G.; Hoffmann, M. R. *Mol. Phys.* **2009**, *107*, 889−897.
(91) Helgaker, T.; Klopper, W.; Koch, H.; Noga, J. *J. Chem. Phys.* **1997**, *106*, 9639−9646.
(92) Halkier, A.; Helgaker, T.; Jørgensen, P.; Klopper, W.; Koch, H.; Olsen, J.; Wilson, A. K. *Chem. Phys. Lett.* **1998**, *286*, 243−252.
(93) Schwartz, C. *Phys. Rev. A* **1962**, *126*, 1015−1019.
(94) Gingerich, K. A. *Faraday Symp. Chem. Soc.* **1980**, *14*, 109−125.
(95) Xu, X.; Truhlar, D. G. *J. Chem. Theory Comput.* **2012**, *8*, 80−90.
(96) Roos, B. O.; Borin, A. C.; Gagliardi, L. *Angew. Chem., Int. Ed.* **2007**, *46*, 1469−1472.
(97) Brynda, M.; Gagliardi, L.; Roos, B. O. *Chem. Phys. Lett.* **2009**, *471*, 1−10.
(98) Andersson, K. *Chem. Phys. Lett.* **1995**, *237*, 212−221.
(99) Bunge, C. F.; Barrientos, J. A.; Bunge, A. V. *At. Data Nucl. Data Tables* **1993**, *53*, 113−162.